International Journal of Nanomedicine

Dovepress
Taylor & Francis Group

Open Access Full Text Article

ORIGINAL RESEARCH

Si-ITGA6-Loaded Liposomes Inhibit Capsule Fibrosis via the FAK/PI3K/Akt Signaling Pathway in Adhesive Capsulitis of Shoulder

Beijie Qi[1,*], Qi Wang[1,*], Shi Shi[1,*], Qian Wang[1,*], Weihao Jiang[1], Chenxu Wang[2], Dejian Li[1], Yaying Sun[3], Chengqing Yi[1]

[1]Department of Orthopedics, Shanghai Pudong Hospital, Fudan University Pudong Medical Center, Shanghai, People's Republic of China; [2]Department of Orthopedics, The First Affiliated Hospital of Henan University, Kaifeng, Henan, People's Republic of China; [3]Department of Sports Medicine, Shanghai General Hospital, Shanghai Jiao Tong University School of Medicine, Shanghai Jiao Tong University, Shanghai, People's Republic of China

*These authors contributed equally to this work

Correspondence: Chengqing Yi; Yaying Sun, Email chengqingyi100@163.com; yaying.sun@shgh.cn

Background: Adhesive capsulitis of shoulder (ACS) is a common shoulder disease with pain, joint stiffness, and capsule fibrosis. The pathogenesis of ACS remains unclear, and long-term efficacy of current treatment for ACS is not satisfactory. Given the absence of targeted therapy, proteomic analysis is conducted on the capsules of ACS patients, in an effort to identify the potential target for ACS treatment. The liposome-based siRNA delivery system was utilized for in vivo experiments due to its non-immunogenicity, stability, and low off-target effects compared to other siRNA delivery methods. We aimed to provide a potential approach for targeted therapy of ACS.

Methods: Capsules from rotator cuff tear (RCT) patients with or without ACS were collected. Proteomic analysis was performed to detect differentially expressed proteins. For in vitro experiments, EdU assay, wound healing assay, CCK-8, quantitative polymerase chain reaction, immunofluorescence staining and western blot was conducted. Histological, immunofluorescence and biomechanical assessments were utilized in a mouse model of ACS. The properties of siRNA-loaded liposomes were determined using laser particle size analyzer and electron microscopy.

Results: Proteomic analysis identified integrin α6 (ITGA6) as a significantly upregulated protein in the capsules of RCT patients with ACS compared to those without ACS. ITGA6 promoted cell proliferation, migration ability, and pro-fibrotic proteins expression, while the blockade of ITGA6 exhibited anti-fibrotic effect. The regulatory effect of ITGA6 was dependent on FAK/PI3K/Akt signaling pathway. Finally, liposome was prepared to carry si-ITGA6, and this si-ITGA6-loaded liposomes demonstrated a potent therapeutic effect in a mouse model of ACS. After si-ITGA6-loaded liposomes injection, the capsule thickness was decreased from 120.3 ± 14.3 μm to 73.3 ± 12.6 μm ($p < 0.01$), and the ROM also improved from 81.0 ± 9.0 to 112.2 ± 8.1 degrees ($p < 0.01$). These results indicated that si-ITGA6-loaded liposomes significantly ameliorated capsule fibrosis and joint mobility without indication of toxicity.

Conclusion: This research elucidated that ITGA6 was upregulated in the capsules of patients with ACS and is capable of significantly activating fibroblasts through the FAK/PI3K/Akt signaling pathway. By targeting ITGA6, si-ITGA6-loaded liposomes could effectively attenuate capsule fibrosis. In this study, we identified ITGA6 as a key regulator in ACS and demonstrated that targeting ITGA6 with siRNA-loaded liposomes effectively attenuated capsule fibrosis and improved joint mobility, offering a promising approach for targeted therapy of ACS.

Keywords: adhesive capsulitis, integrin α6, fibrosis, liposome

Introduction

Adhesive capsulitis of shoulder (ACS) is a common shoulder disease characterized by persistent pain and shoulder stiffness (SS), particularly with limitation in range of motion (ROM).[1] ACS typically progresses through three stages: pain phase, frozen phase, and thawing phase. ACS is classified into primary and secondary forms based on the presence

Received: 18 October 2024
Accepted: 31 March 2025
Published: 5 April 2025

of an identifiable etiology. Primary ACS manifests spontaneously without any evident precipitating factors, with an incidence rate of 2–5%, predominantly affecting individuals aged 40–60, and with a higher prevalence in females than in males.[2] Secondary ACS, on the other hand, is generally caused by other diseases including systemic diseases, surgery or trauma, infections and metabolic disorders.[3] The specific mechanisms underlying the pathogenesis of ACS remain yet unclear.

The primary pathological manifestations of ACS include chronic inflammation, capsular contracture, and capsular fibrosis.[4,5] A large number of researches indicate that fibroblasts play a critical role in the process of ACS.[6] Joint capsule fibrosis is highly associated with the recruitment, proliferation, and activation of fibroblasts.[7] Triggered by inflammation, cytokines accumulate locally, recruiting and activating fibroblasts into α-SMA (+) myofibroblasts, which leads to excessive secretion of collagen in the extracellular matrix (ECM). The overaccumulation of collagen, in turn, further triggers the occurrence of fibrosis.[8] Hettrich et al found that the capsules in ACS showed a higher level of myofibroblasts compared to capsules in control group.[9] Akbar et al provided evidence that fibroblasts in ACS became activated and secreted the higher prevalence of inflammatory cytokines, such as IL-6 and IL-8 et al.[10] These findings substantiate a close association between fibroblast activation and ACS. On the ground of this, attenuating excessive proliferation and activation of fibroblasts is an important measure for alleviating capsular fibrosis in ACS.

Current therapeutic approaches for ACS include physical therapy, oral non-steroidal anti-inflammatory drugs (NSAIDs), intra-articular glucocorticoid injection, surgical release, and traditional Chinese medicine therapy.[11,12] However, there is still no consensus on the treatment for ACS, and the long-term efficacy of these treatments, as well as their effectiveness at different stages of ACS, remain to be verified.[13] Therefore, further research into the pathogenesis of ACS and its underlying mechanisms to improve pain and SS is an urgent need.

Proteomics is a crucial technology for studying the totality and characteristics of proteins within organisms. It involves a comprehensive analysis of the protein expression level, structure, function, and interaction with other proteins, playing an essential role in understanding the pathogenesis and progression of various diseases, identifying potential biomarkers, and finding the therapeutic targets.[14,15] Proteomics is an important technique in elucidating the pathogenesis of ACS. By examining the protein expression profiles of clinical samples, researchers have already identified several potential therapeutic targets for various diseases,[16–18] demonstrating that proteomic technology is instrumental in discovering molecular markers, thereby advancing our understanding of ACS and facilitating the development of targeted therapy. Currently, the specific molecular mechanisms underlying the development of ACS and its potential therapeutic targets remain unclear, and few studies have conducted proteomic analysis on the shoulder joint capsule tissues of patients with ACS.

Therefore, our aim is to identify a potential pathogenic protein associated with ACS using proteomic technology and to validate its functions in ACS through in vivo and in vitro experiments. Ultimately, exploring this protein as therapeutic targets to investigate the efficacy of targeted treatments, providing a novel therapeutic approach in ACS.

In the current study, we found that the integrin α6 (ITGA6) expression was significantly upregulated in the joint capsules of patients with ACS. This finding was further validated in TGF-β stimulated NIH3T3s and mouse ACS model. The integrins, a family of transmembrane receptors, have been found to be involved in the development and progression of a variety of fibrotic diseases,[19,20] which was consistent with the findings of this study. In vitro experiments demonstrated that silencing ITGA6 with si-ITGA6 notably inhibited the activity of fibroblasts via FAK/PI3K/Akt signaling pathway. To further investigated the therapeutic effect of si-ITGA6 for ACS targeted treatment, we utilized liposomes to encapsulate si-ITGA6 for the treatment in mouse ACS model, revealing that si-ITGA6-loaded liposomes significantly ameliorated capsule fibrosis in ACS mice. Encapsulating siRNA with liposomes could enhance its stability, protect siRNA from degradation, and facilitate targeted delivery, thereby improving therapeutic efficacy and reducing off-target effects.[21–23] These results suggested the crucial role of ITGA6 in the pathogenesis of ACS and might serve as a potential therapeutic target.

Materials and Methods

Institutional ethical committee of Shanghai Pudong Hospital approved this study (2022-RS-MS-06). All patients signed informed consent for shoulder capsule samples collection and fibroblasts extraction. This study was organized following

the Declaration of Helsinki. The Institutional Animal Care and Use Committee of Shanghai Pudong Hospital approved all animal procedures in the current study (20231011-01). All procedures were conducted following the Guide for the Care and Use of Laboratory Animals.

Patient Inclusion and Sample Collection

Rotator cuff tear (RCT) patients with or without SS were selected in line with the published criteria.[24] The definition of SS was deficiency of passive ROM greater than 25% in flexion, external rotation, and internal rotation in affected joint than counterpart.[25,26] RCT patients accompanied by SS were categorized into the RCT + SS group, and patients with RCT not accompanied by SS were categorized into the RCT group. Baseline data and disease-related data of the two groups including duration and ROM were collected. The patient capsule samples were collected during surgery for further analysis or to extract capsular derived fibroblasts (CDFs) according to previous research.[27]

4D Label-Free Proteomic Analysis

A total of 6 shoulder capsule samples (3 for RCT group and 3 for RCT + SS group) were collected with liquid nitrogen and transferred into 2 mL centrifuge tubes. SDT buffer and quartz sand were subsequently added. The samples were homogenized using an automated homogenizer. The homogenate underwent sonication, boiling, and centrifugation. The supernatant was filtered using 0.22 μm filters. Each sample containing 20 μg proteins. After boiling, samples were separated on SDS-PAGE gel.

For further analysis, each sample containing 100 μg proteins was mixed with DTT. After removing components with low molecular weight, iodoacetamide was added to block reduced cysteine residues. Proteins were digested with trypsin in $NH_4HCOsci_3$ buffer overnight. The peptides were desalted and detected using UV spectral (280 nm).

Samples were analyzed using a nanoElute. Peptides were separated on an analytical column. The column oven temperature was 50°C. After that, samples were loaded in FA and separated with a linear gradient. MS data was processed with MaxQuant (uniport_homo_20221024_20402_9606_swiss_prot). Fold change ≥2 and $p < 0.05$ were considered as differentially expressed proteins.

Cell Culture

Both CDFs and NIH3T3s were incubated in high-glucose DMEM medium (Servicebio, China) supplemented with 10% fetal bovine serum (C0235, Beyotime) plus 1% penicillin/streptomycin (NCM Biotech, China). CDFs harvested from the capsule were considered as passage 0. Both CDFs and NIH3T3s were passaged when the confluence reached 90%. CDFs were used for subsequent experiments at passage 3. Both CDFs and NIH3T3s were incubated at 37°C with 5% CO_2.

Cell Interventions

When cells (CDFs or NIH3T3s) reached confluence of 80%, the growth medium was replaced. Cells were stimulated by transforming growth factor-β (TGF-β, 20 ng/mL) for 1d.

Cell transfection was conducted with Advance Transfection Reagent (Zeta Life, USA). About 60 nM small interfering RNAs against ITGA6 (si-ITGA6) and pCDH-ITGA6 plasmid were obtained from RiboBio (Guangzhou, China). LY294002 was purchased from MedChemExpress (MCE, USA) and was utilized to inhibit PI3K/Akt signaling pathway.

Hematoxylin & Eosin (HE) Staining

The procedure of HE staining was conducted according to a previous study.[28] In detail, the shoulder joint tissues were embedded and sliced into sections, then underwent dewaxing and rehydration. Next, hematoxylin and eosin staining were performed. After staining, slices were sealed by neutral resin and pictured with microscope (LEICA DM2500).

Masson's Trichrome Staining

Embedded tissues were sliced into sections and then dewaxed and rehydrated. Next, Masson staining was performed with Masson Stain Kit (Servicebio, China). After staining, neutral resin was utilized to seal the sections, and sections were

observed and pictured using microscope (LEICA DM2500). Meanwhile, joint capsule thickness was measured, and cell count was determined within an area of 25 μm×25 μm (each sample was counted five times).

Immunofluorescence Staining

The details of antibodies were demonstrated in Table S1. The procedure of immunofluorescence staining was described previously.[28] Embedded tissues were sliced into sections and then dewaxed and rehydrated. CDFs or NIH3T3s were treated with fixing solution (P0098, Beyotime). Next, capsule sections and cells were subsequently treated with blocking buffer (P0260, Beyotime). Following this, sections and cells were sequentially incubated with corresponding primary and secondary antibodies (ab150077, ab150116, Abcam). DAPI was utilized to stain the nucleus in CDFs and NIH3T3s. Sections and cells were observed and pictured by the fluorescence microscope (Zeiss Axio Observer 7).

Sirius Red Staining

After cutting, dewaxing, and rehydration, Sirius red staining was performed with a Modified Sirius Red Stain Kit (G1472, Solarbio). In brief, sections were stained with iron hematoxylin solution for 5 min. Then Sirius red staining solution was administered on sections for 15 min. After washing, dehydration, and sealing, capsule samples were observed and imaged by a microscope (LEICA DM2500) with a polarized lens.

Western Blot (WB)

Proteins were obtained from CDFs/NIH3T3s or capsule samples with RIPA lysis buffer (WB3100, NCM Biotech) containing PMSF. Then proteins were separated on gels, followed by transferring to PVDF membranes. After blocking, blots were incubated with corresponding primary and secondary antibodies. Finally, all blots were observed and pictured with ChemiDoc MP Imaging System (12003154, Bio-Rad).

Quantitative Polymerase Chain Reaction (qPCR)

RNA Purification Kit (B0004DP, EZBioscience) was utilized to obtain RNA from cells. Then, the RNA concentration was analyzed by NanoDrop spectrophotometer (ThermoFisher, USA). Afterwards, RNA was reverse-transcribed to complementary DNA with HyperScript^{TM} III RT SuperMix kit (R202, EnzyArtisan). The SYBR qPCR Mix kit (Q204, EnzyArtisan) was utilized for amplification. Afterwards, the PCR analysis was conducted with ViiA^{TM} 7 Real-Time PCR System (4453535, ThermoFisher). The mRNA qPCR primers were demonstrated in Table S2. Data were quantified by the $2^{-\Delta\Delta Ct}$ method.

EdU Cell Proliferation Assay

Cells were treated with a 1 mL EdU (10 μM) solution for 2 h in each well to label cells. Next, cells were treated with fixing solution (P0098, Beyotime) for 10 min and subsequently treated with 0.3% Triton X-100 and click reaction regent. DAPI was utilized to stain the nucleus. At last, petri dishes were observed and pictured using the fluorescence microscope (Zeiss Axio Observer 7).

Wound Healing Assay

Wound healing assay was conducted by creating a straight scratch in the center of 6-well plates with a 200 μL pipette tips when cells reached a confluence of 80%. Next, corresponding interventions were administered, and petri dishes were observed and imaged using the microscope (LEICA DM2500). The migration ability of cells was calculated based on the recovery rate.

CCK-8 Assay

Cell viability of CDFs or NIH3T3s under various conditions was analyzed with CCK-8 reagent kit (HY-K0301, MCE). In detail, cells were seeded and various interventions were conducted for 1 d. Next, cells were incubated with CCK-8 reagent for 2 h. After that, 96-well plates were detected by microplate reader (Varioskan LUX, Thermo Scientific) with the absorbance of 450 nm.

Preparation and Characterization of Si-ITGA6-Loaded Liposomes

Liposome was utilized to encapsulate siRNA. The procedure of liposome preparation was performed as previous study.[29] Liposomes were composed of lipid, cholesterol, DSPC, and mPEG-DMG in a molar ratio of 50:38.5:10:1.5. Simultaneously, siRNA was added into citrate buffer and mixed with the lipid solution. After removing unentrapped siRNA, liposome morphology was detected using transmission electron microscopy (TEM). The encapsulation efficiency was detected by spectrofluorometer (Infinite M200 PRO, Tecan). The characterization of liposomes was investigated with laser particle size analyzer (90 Plus, Brookhaven).

Establishment of Mice Adhesive Capsulitis Model

Male C57/6J mice were utilized in this study. Adhesive capsulitis model was established by shoulder joint immobilization according to previous studies.[30,31] Intra-articular injection of PBS or liposomes was administered one week and two weeks after the surgery with a micro-syringe.

All animals were allowed to move freely and get access to food under a 12 h light–dark circle condition after surgery. Mice in NC group underwent sham surgery. Mice underwent immobilization operation and PBS injection were categorized as Model group. Those underwent immobilization operation plus empty liposomes or si-ITGA6-loaded liposomes injection were categorized as Model + liposomes group or Model + si-ITGA6 liposomes group.

Three weeks after the model was established, all mice were euthanized with overdose CO_2 and shoulder samples were harvested. The ROM was measured according to published research.[32] All measurements were performed by a researcher who was unaware of the group assignments.

Furthermore, another 12 mice were allocated to each group to evaluate the toxicity of liposomes in vivo. Major organs were harvested to assess any morphological abnormalities.

Statistical Analysis

GraphPad Prism software was utilized for statistical analysis. Quantitative data were presented as mean ± SD. The differences between groups were assessed using Student's *t*-test or one-way analysis of variance. $p < 0.05$ was regarded statistical significance.

Results

ITGA6 Was Significantly Upregulated in Capsules from Patients with ACS

Six samples were collected, three in RCT group and three in RCT + SS group. Detailed demographic data and passive ROM was presented in Table 1. No significant difference was found in basic features between two groups. However, passive ROM in RCT + SS group was remarkably lower than RCT group, indicating a significant stiffened status of shoulder joint.

Table 1 Basic Characteristics of Patients Enrolled

Items	Group RCT (n=3)	Group RCT+SS (n=3)	p value
Sex (male/female)	1/2	1/2	1.000
Age (year)	58.3±14.7	53.3±8.7	0.700
Height (cm)	161.9±3.1	163.2±4.9	0.706
Weight (kg)	63.3±7.0	67.1±5.2	0.502
Duration (month)	6.0±5.3	3.7±2.1	0.517
Flexion (degree)	156.7±15.3	100.0±17.3	0.013
Abduction (degree)	151.7±16.1	76.7±11.5	0.003
External rotation at side (degree)	73.3±5.8	11.7±2.9	<0.001
Internal rotation at back*	5.0±2.0	16.3±1.5	0.002

Notes: *: Vertebra level was numbered serially 1 to 12 for the 1st to 12th thoracic vertebrae, 13–17 for the 1st to 5th lumbar vertebrae, and 18 for below the sacral region.
Abbreviations: RCT, rotator cuff tear; SS, shoulder stiffness.

https://doi.org/10.2147/IJN.S501561

Next, shoulder capsule samples were collected, and proteomic analysis was conducted between RCT + SS group and RCT group. The levels of differentially expressed proteins (DEPs) were presented by volcano plot (Figure 1A) after screening (fold change ≥ 2, $p < 0.05$). The expression profiling data demonstrated 64 DEPs in total, with 42 upregulated and 22 downregulated. In addition, the KEGG analysis presented the top 20 most enriched pathways (Figure 1B). Among these, ECM–receptor interaction, focal adhesion, and PI3K-Akt signaling pathway played critical role in the fibrogenesis process. Venn diagram analysis of the DEPs enriched in these three signaling pathway resulted in the identification of the following five DEPs: LAMC1, LAMB2, LAMA4, LAMA5, and ITGA6 (Figure 1C). Among these, LAMC1, LAMB2, LAMA4, and LAMA5 were laminins, which were proteins of the extracellular matrix family widely presented in the organism. ITGA6, or integrin α6, is a type of cell membrane receptor that participates in different cellular functions such as cell adhesion and proliferation, and evidence shows that the integrin family is involved in the progression of various fibrosis-related diseases.[33–35] This information indicated that ITGA6 might be engaged in the fibrotic process of ACS. Therefore, ITGA6 was selected as a key target for subsequent research.

HE staining of capsules showed a higher level of cell infiltration in RCT + SS group, and Masson staining suggested more extensive collagen deposition in RCT + SS group than RCT group (Figure 1D). WB and immunofluorescence staining demonstrated that the level of pro-fibrotic proteins, Col 1 and α-SMA, were significantly upregulated in the capsules of RCT + SS group compared to RCT group (Figure 1E–H). These results indicated that the joint capsules of patients with ACS underwent significant fibrosis, consistent with the passive ROM data mentioned before. Additionally, we detected a significant upregulation of ITGA6 in the joint capsules of ACS patients by WB and immunofluorescence (Figure 1E, F, I and J), which was also in line with the observation of proteomic analysis.

ITGA6 Was Upregulated in Mouse Capsules of ACS Model and NIH3T3 Cells Stimulated with TGF-β

After confirming the upregulation of ITGA6 expression in the capsules of ACS patients, we further validated the expression of ITGA6 in a mouse ACS model. Prominent cell infiltration and significantly thickened capsules were observed in the Model group than in NC group by HE staining (Figure 2A–C). In addition, Sirius red staining detected a remarkable collagen deposition in capsule of Model group (Figure 2A and D). Correspondingly, the ROM in Model group was remarkably lower than NC group (Figure 2E). The expression of α-SMA and Ki67 significantly accumulated in the capsules of Model group than that of NC group (Figure 2F–H). These results suggested the successful establishment of the mouse ACS model, characterized by significant thickening, stiffness, and fibrosis of the joint capsules. Base on this, we measured the expression of ITGA6 in vivo. Immunofluorescence staining revealed that the ITGA6 expression in the capsules of Model group was remarkably higher (Figure 2I and J), which was consistent with the results obtained from the capsules of patients with ACS as mentioned earlier.

To mimic the fibrotic circumstance in vitro, NIH3T3 fibroblasts were stimulated by TGF-β. Immunofluorescence staining results demonstrated that under the stimulation of TGF-β, ITGA6 significantly upregulated in NIH3T3s (Figure S1A and B). EdU assay showed the enhanced cell proliferation activity in TGF-β group (Figure S1C and D) and significantly increased expression of α-SMA and Col 1 was detected in TGF-β group than that in NC group by immunofluorescence staining (Figure S1E–G). These findings convincingly demonstrated that ITGA6 was significantly upregulated under fibrotic conditions. However, whether ITGA6 was involved in the regulation of fibroblast activity still required further confirmation.

Knockdown of ITGA6 Attenuated TGF-β Induced Fibrogenesis in vitro

To investigate the regulatory effect of ITGA6 on fibroblast activity, three siRNAs targeted ITGA6 were constructed, and one with the best knockdown efficiency (si-ITGA6-2) was selected (Figure 3A). Additionally, in order to make the experimental results more convincing, capsule-derived fibroblasts (CDFs) were extracted from capsule samples of RCT patients. Immunofluorescence staining (Figure 3B and C) and WB (Figure 3D and E) showed that ITGA6 expression was significantly upregulated after stimulation of TGF-β, while si-ITGA6 remarkably attenuated the expression levels of ITGA6 under TGF-β stimulation, indicating the high knockdown efficiency of si-ITGA6. In addition, we found that the proliferation and migration

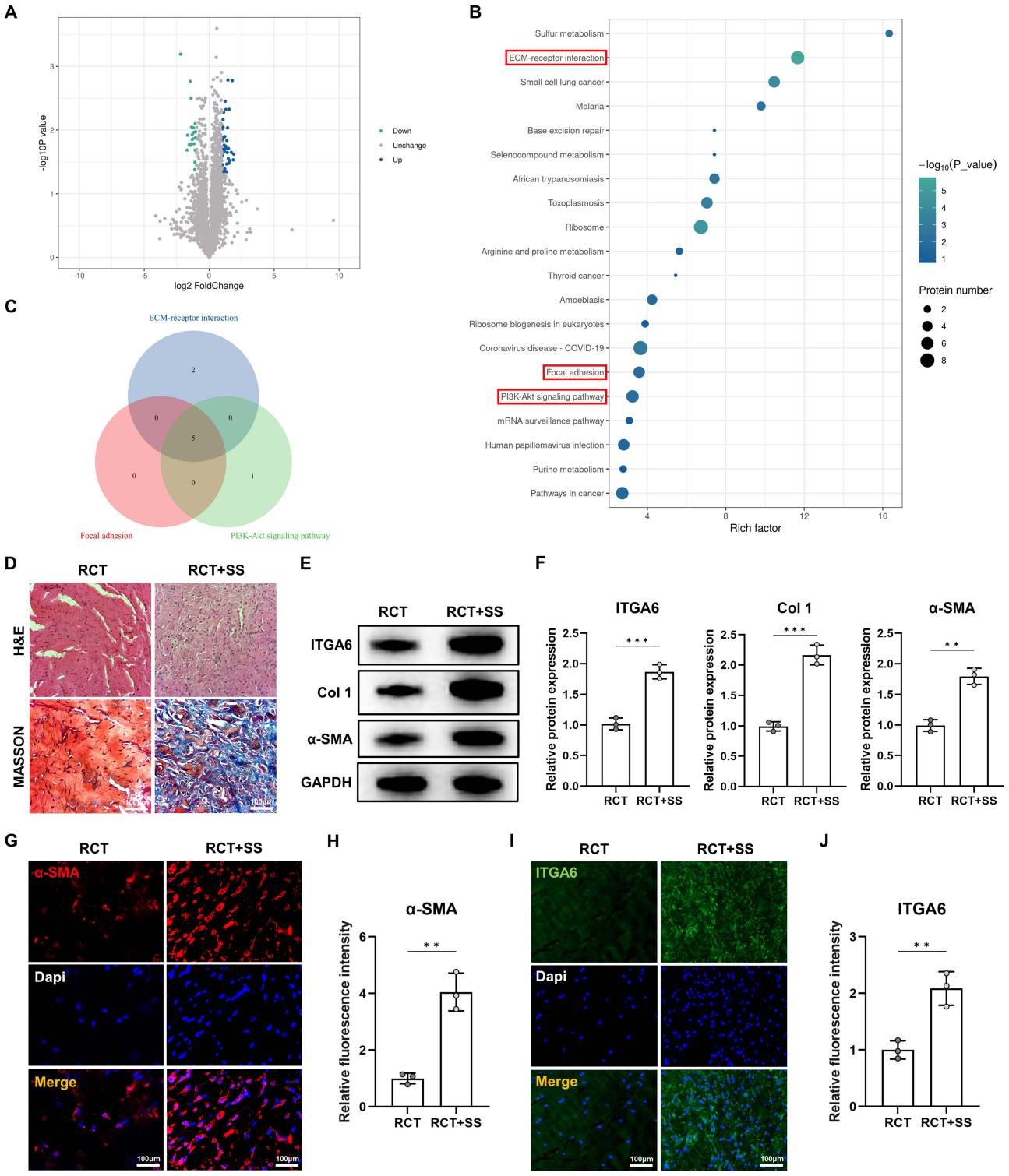

Figure 1 ITGA6 was upregulated in capsules of patients with ACS. (**A**) Volcano plot diagram demonstrated the DEPs between capsule samples from ACS patients with or without SS. (**B**) KEGG pathway analysis displayed the top 20 most enriched signaling pathways. (**C**) Venn diagram illustrated the intersection of DEPs in ECM–receptor interaction, focal adhesion, and PI3K-Akt signaling pathways. (**D**) Representative HE and Masson staining images demonstrated significant cell infiltration and collagen deposition in the capsules of ACS patients with SS compared to those without SS. (**E** and **F**) Western blot showed the expression of ITGA6, Col 1, and α-SMA in capsules from RCT patients with or without SS. (**G** and **H**) Immunofluorescence analysis of α-SMA in capsules from RCT patients with or without SS. (**I** and **J**) Immunofluorescence analysis of ITGA6 in capsules from RCT patients with or without SS. **p < 0.01, ***p < 0.001.

https://doi.org/10.2147/IJN.S501561

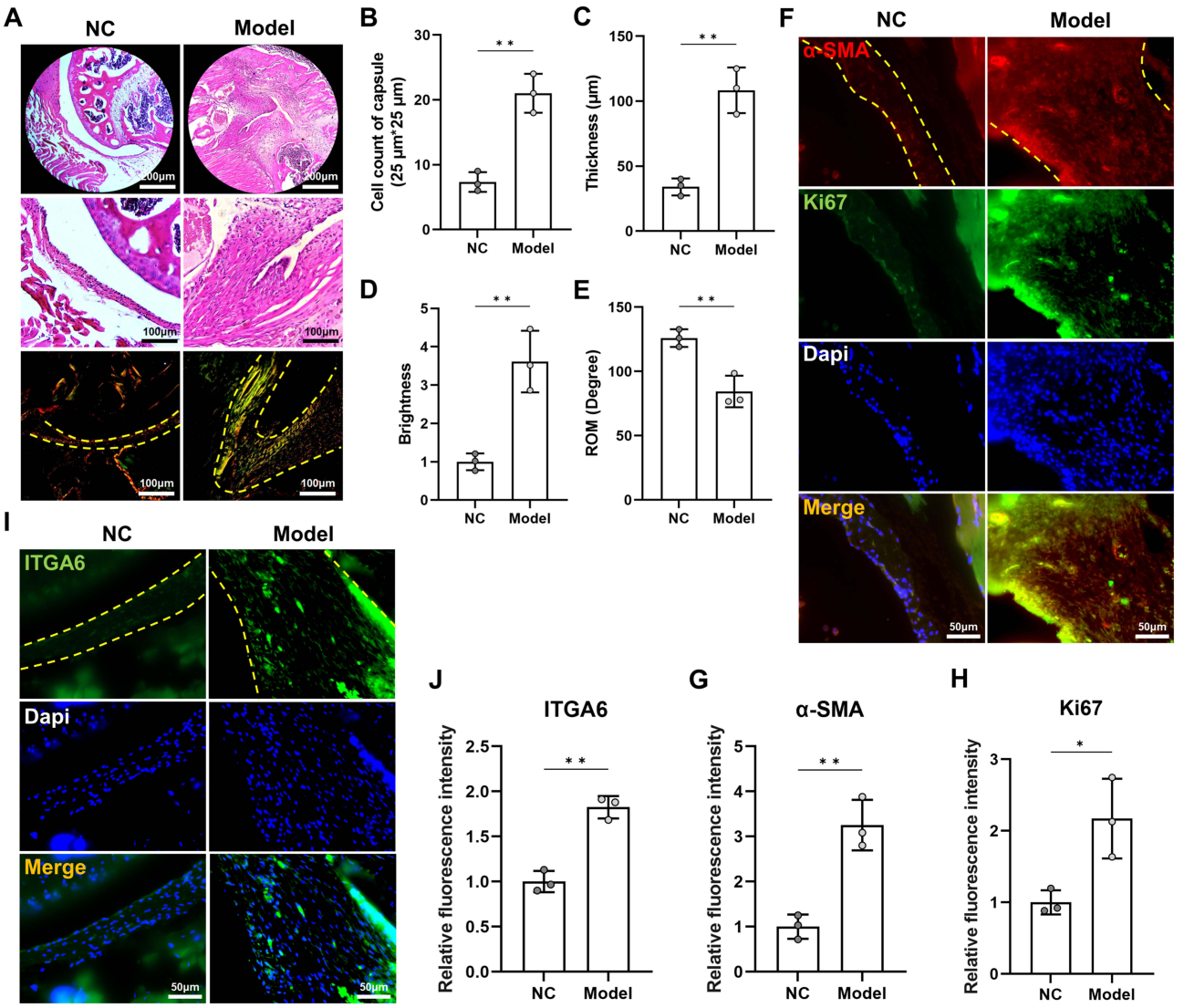

Figure 2 ITGA6 was upregulated in capsules of mice ACS model. (**A**) Representative HE and Sirius red staining images of the shoulder capsules in different group. The outline of the capsules was marked with yellow dashed lines. (**B**) Cell number count in capsules of different groups. (**C**) Average capsule thickness in different groups. (**D**) Relative collagen deposition in capsules of different groups. (**E**) Passive ROM of mice shoulder in different groups. (**F–H**) Immunofluorescence analysis of α-SMA and Ki67 in shoulder capsules. (**I** and **J**) Immunofluorescence analysis of ITGA6 in shoulder capsules. *p < 0.05, **p < 0.01.

activity of CDFs were significantly upregulated by TGF-β, while knockdown of ITGA6 significantly prohibited TGF-β-induced CDFs activity by EdU, wound healing, and CCK-8 assay (Figure S2A–E). Correspondingly, WB (Figure 3D and F–H) and immunofluorescence staining (Figure 3I–K) presented a significant down-regulation of Col 1, VIM, and α-SMA expression after ITGA6 knockdown in CDFs stimulated with TGF-β. These findings were also replicated in NIH3T3s (Figure S3). These findings indicated the activating role of ITGA6 on fibroblasts.

FAK/PI3K/Akt Signaling was Involved Both in Capsules from ACS Patients and CDFs Stimulated with TGF-β

Upon clarifying the regulatory role of ITGA6 on the activity of fibroblasts, we investigated the specific mechanisms by which ITGA6 regulated CDFs. Results from the KEGG pathway enrichment analysis revealed a high enrichment of DEPs in PI3K-Akt signaling (Figure 4A). FAK/PI3K/Akt signaling is well known to activate fibroblasts in various fibrotic diseases.[35,36] Our validation using immunofluorescence staining (Figure 4B and C) also showed that p-Akt expression in capsules of RCT + SS group was significantly higher than RCT group. Subsequently, we examined the activity of FAK/PI3K/Akt signaling in CDFs.

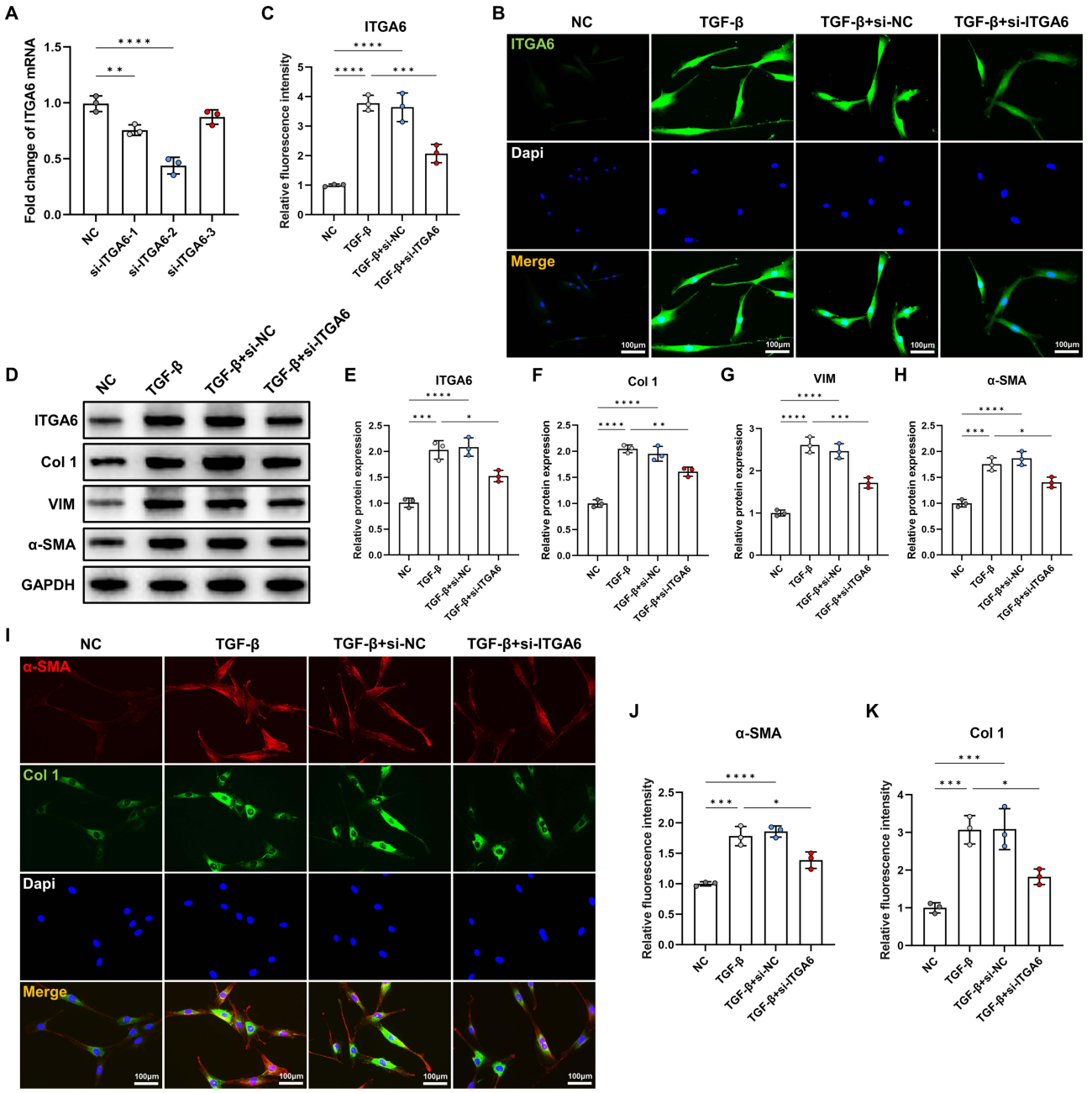

Figure 3 Si-ITGA6 attenuated fibrogenesis induced by TGF-β. (**A**) Relative ITGA6 gene expression level detected by qPCR. (**B** and **C**) Immunofluorescence analysis of ITGA6 in CDFs after different treatment. (**D–H**) Western blot showed the expression of ITGA6, and pro-fibrotic proteins Col 1, VIM, and α-SMA in CDFs. (**I–K**) Immunofluorescence analysis of α-SMA and Col 1 in CDFs after different treatment. *p < 0.05, **p < 0.01, ***p<0.001, ****p < 0.0001.

WB results (Figure 4D–G) indicated that the activity of p-FAK, p-PI3K, and p-Akt was significantly stimulated by TGF-β. Similarly, an upregulation of p-Akt in TGF-β stimulated CDFs was observed by immunofluorescence staining (Figure 4H and I). Notably, si-ITGA6 significantly inhibited the TGF-β-induced activation of FAK/PI3K/Akt signaling pathway in CDFs (Figure 4D–I). These results demonstrated the activation of FAK/PI3K/Akt signaling in capsules of ACS patients and activated CDFs.

ITGA6 Affected the Activation of CDFs Through FAK/PI3K/Akt Signaling

Next, we questioned if ITGA6 regulated the pro-fibrotic phenotype via the aforementioned pathway. We constructed pCDH-ITGA6 plasmids to overexpress ITGA6 in CDFs. After transfected with pCDH-ITGA6 plasmids, p-Akt was

https://doi.org/10.2147/IJN.S501561

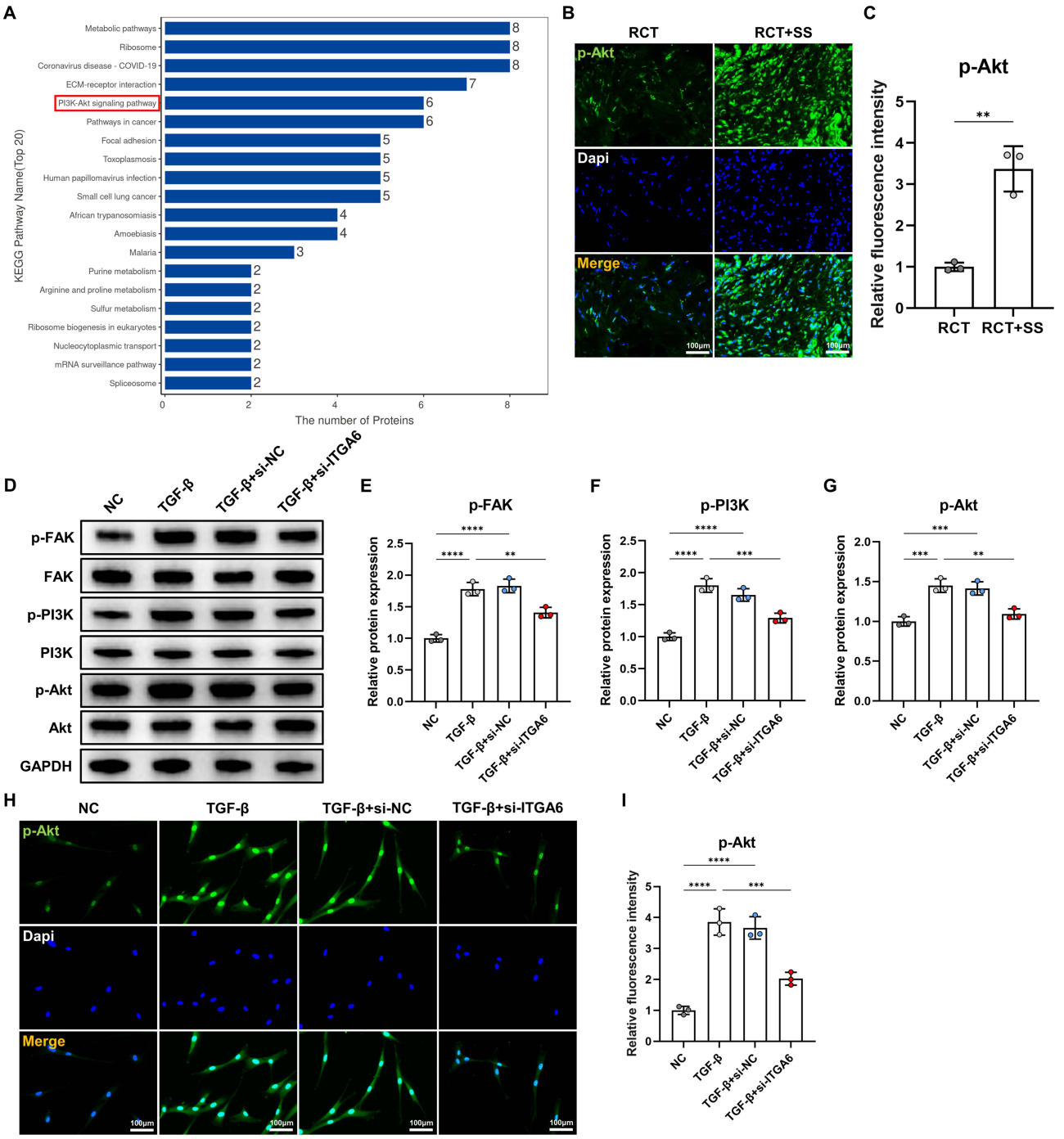

Figure 4 PI3K-Akt signaling was involved in capsules of ACS patients and TGF-β stimulated CDFs. (**A**) KEGG analysis displayed the top 20 most enriched signaling pathways. (**B** and **C**) Immunofluorescence analysis of p-Akt in capsules of RCT patients with or without SS. (**D**–**G**) Western blot showed the expression of p-FAK, p-PI3K, and p-Akt in CDFs. (**H** and **I**) Immunofluorescence analysis of p-Akt in CDFs after different treatment. **p < 0.01, ***p<0.001, ****p < 0.0001.

significantly upregulated in CDFs compared to NC group, as presented by immunofluorescence staining (Figure 5A and B). WB also demonstrated that the p-FAK, p-PI3K, and p-Akt were remarkably increased (Figure 5C and D). EdU assay suggested that the cell proliferation ability was significantly promoted by pCDH-ITGA6 (Figure S4A and B). In addition, the fibrotic phenotypes of CDFs treated with pCDH-ITGA6 plasmids were assessed. Immunofluorescence staining indicated that the pCDH-ITGA6 significantly upregulated α-SMA and Col 1 (Figure 5E–G), indicating the pro-fibrotic

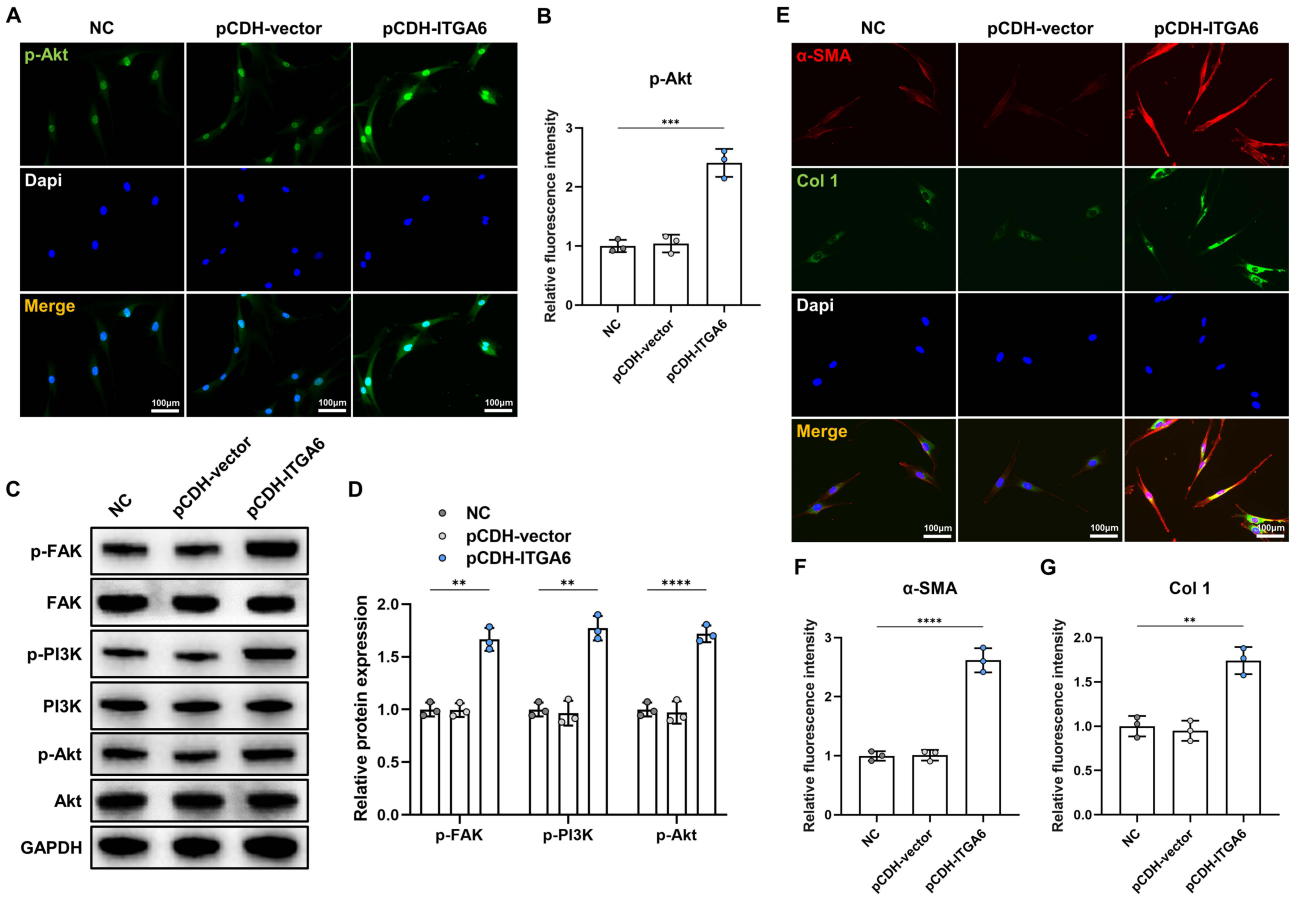

Figure 5 Overexpression of ITGA6 upregulated the phosphorylation level of FAK/PI3K/Akt, as well as the pro-fibrotic markers. (**A** and **B**) Immunofluorescence analysis of p-Akt in CDFs after different treatment. (**C** and **D**) Western blot showed the expression levels of p-FAK, p-PI3K, and p-Akt in CDFs. (**E–G**) Immunofluorescence analysis of α-SMA and Col 1 in CDFs after different treatment. **p < 0.01, ***p < 0.001, ****p < 0.0001.

effect of ITGA6. These results revealed that overexpression of ITGA6 activated the CDFs and the FAK/PI3K/Akt signaling.

Moreover, PI3K-Akt signaling pathway inhibitor, LY294002, was utilized to co-treat CDFs with pCDH-ITGA6. We found that LY294002 could significantly mitigate pCDH-ITGA6-induced activation of PI3K-Akt signaling (Figure 6A–D). EdU assay demonstrated that cell proliferation ability elevated by pCDH-ITGA6 was significantly inhibited by LY294002 (Figure S5A and B). Meanwhile, α-SMA and Col 1 upregulated by pCDH-ITGA6 was also attenuated by LY294002 (Figure 6E–G). Together, these findings suggested that ITGA6 regulated CDFs activity and fibrotic phenotype through or at least partially through FAK/PI3K/Akt signaling pathway.

Generation of Si-ITGA6-Loaded Liposomes and Its Therapeutic Effect in vivo

The above experimental data unveiled that ITGA6 could be a potential therapeutic target for ACS, and thus si-ITGA6 was selected for further treatment in vivo. Considering the efficacy and safety of in vivo drug administration, liposomes were prepared to carry and deliver si-ITGA6 because of their capability of protecting siRNAs from degradation and low toxic effects.[37] The blank liposomes and si-ITGA6-loaded liposomes were synthesized, and the characterization and biocompatibility were sequentially analyzed (Figure 7A).

The morphology of liposomes was detected by TEM, as demonstrated in Figure 7B. The diameter of blank liposomes was 109.02 ± 12.09 nm, while that of si-ITGA6-loaded liposomes was 106.26 ± 7.46 nm. Both liposomes remained stable for at least 24 h (Figure 7C). The PDI of blank liposomes and si-ITGA6-loaded liposomes was 0.17 ± 0.02 and 0.19 ± 0.03, respectively (Figure 7D), and the zeta potential of blank/si-ITGA6-loaded liposomes was 21.74 ± 1.13 mV

https://doi.org/10.2147/IJN.S501561

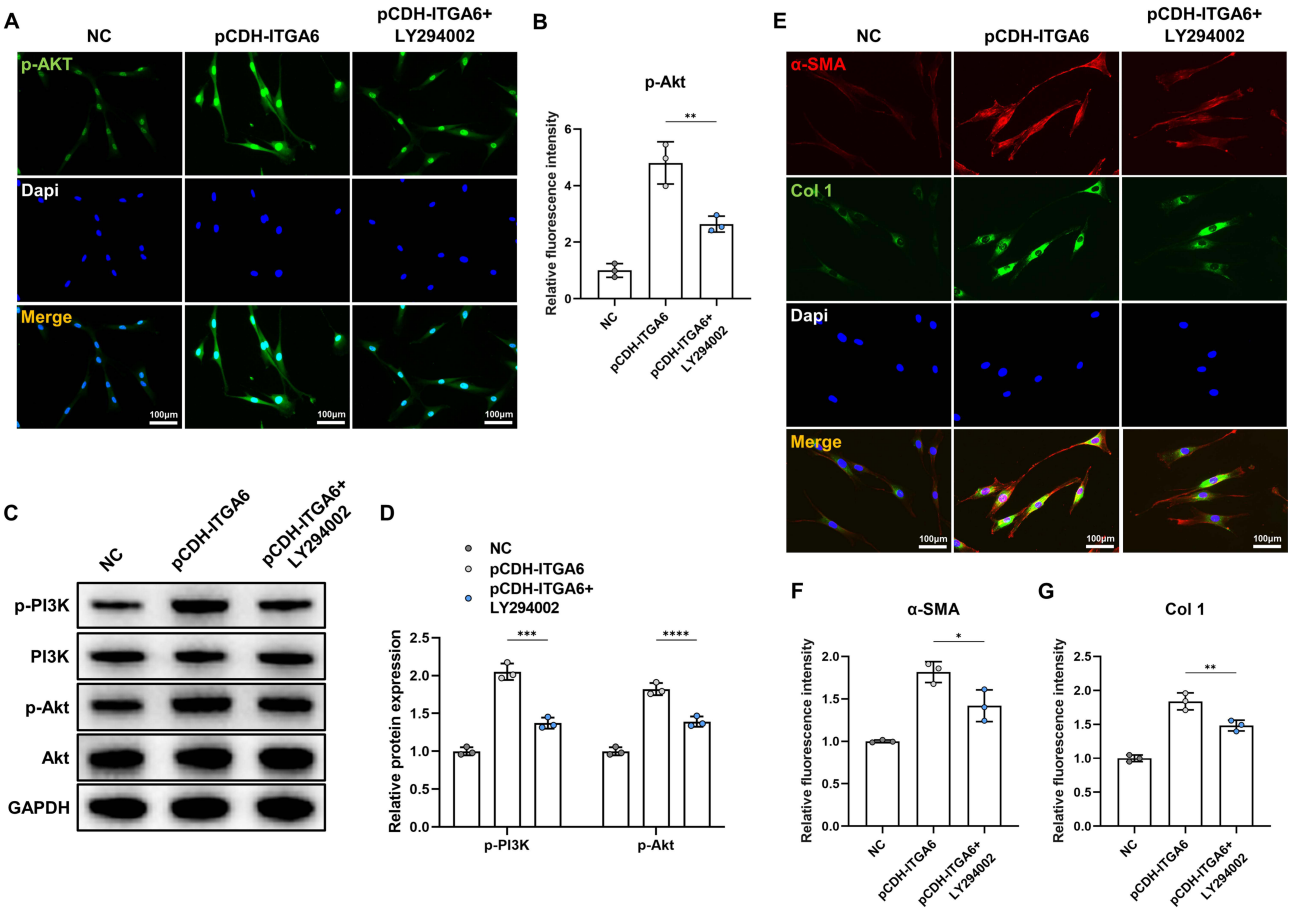

Figure 6 The expression level of p-PI3K, p-Akt, and pro-fibrotic markers upregulated by pCDH-ITGA6 was attenuated by LY294002. (**A** and **B**) Immunofluorescence analysis of p-Akt in CDFs after different treatment. (**C** and **D**) Western blot showed the expression of p-PI3K, and p-Akt in CDFs. (**E–G**) Immunofluorescence analysis of α-SMA and Col 1 in CDFs after different treatment. *p < 0.05, **p < 0.01, ***p<0.001, ****p < 0.0001.

and 2.82 ± 0.05 mV, respectively (Figure 7E). The encapsulation efficiency of si-ITGA6-loaded liposomes was 82.70 ± 1.89%. In addition, the biocompatibility was assessed by CCK-8 assay. The results indicated that there was no significant decrease of NIH3T3s viability when the si-ITGA6-loaded liposomes reached a concentration of 200 nM (Figure 7F).

For experiments in vivo, intra-articular injection of 50 μL si-ITGA6-loaded liposomes at a concentration of 200 nM were administered to the shoulder joint of ACS model mice at one and two weeks after model establishment. Then, shoulder samples were harvested one week after the second injection. Immunofluorescence staining showed that the elevated expression of ITGA6 was successfully attenuated by si-ITGA6-loaded liposomes (Figure S6A and B), indicating that the si-ITGA6-loaded liposomes successfully targeted and inhibited ITGA6 expression in vivo. HE staining and Sirius red staining demonstrated that the si-ITGA6-loaded liposomes remarkably inhibited cell infiltration in capsules, reduced capsule thickness, and attenuated collagen deposition (Figure 8A–D). Passive ROM was also improved by si-ITGA6-loaded liposomes (Figure 8E). Meanwhile, for immunohistology, the expression of α-SMA and Ki67 significantly accumulated in the capsules of Model group, but was remarkably inhibited by si-ITGA6-loaded liposomes (Figure 8F–H). Additionally, as presented by HE (Figure S7A) and Masson (Figure S7B) staining, major organs from mice with liposomes injection showed no significant morphological abnormality compared to those without liposomes injection. Together, these observations supported the potential therapeutic effect of si-ITGA6-loaded liposomes against ACS.

Discussion

In the current study, we collected capsule samples from RCT patients with or without SS, and conducted proteomic analysis to identify the potential therapeutic target ITGA6. Subsequent in vitro experiments revealed the regulatory role

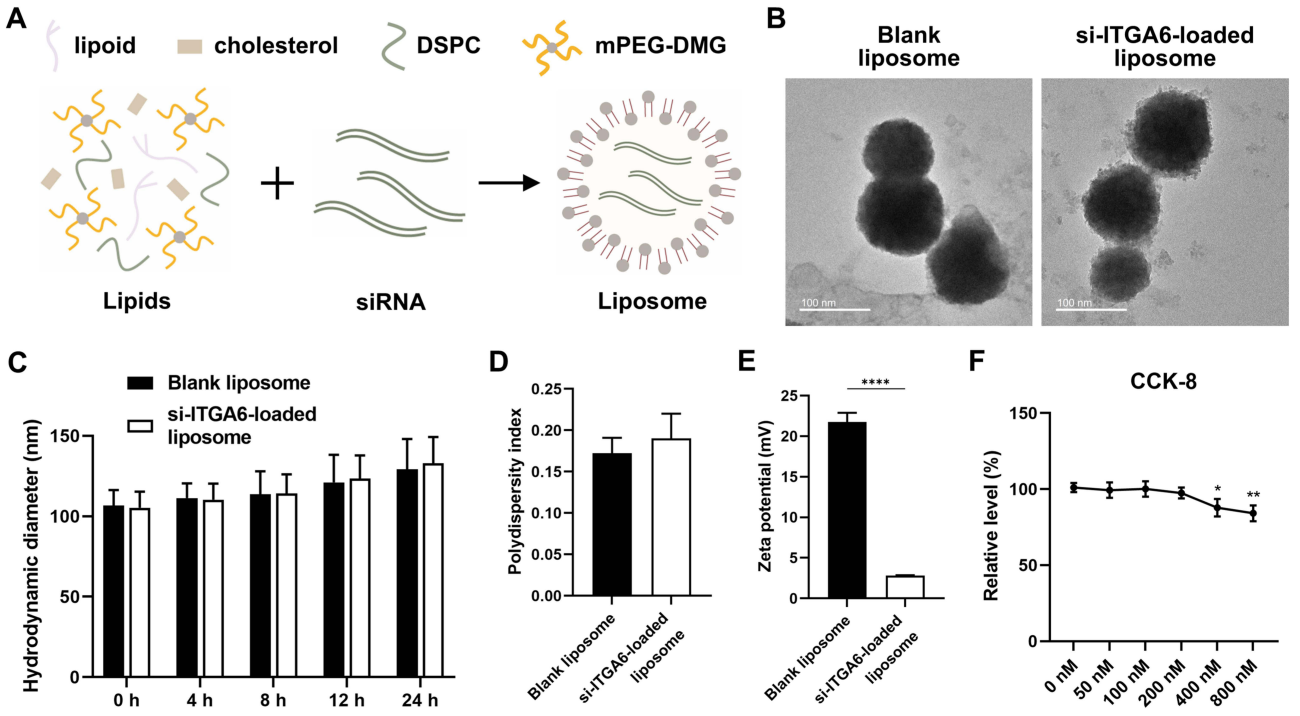

Figure 7 Preparation and characterization of si-ITGA6-loaded liposomes. (**A**) The synthesis of si-ITGA6-loaded liposomes. (**B**) TEM images of blank and si-ITGA6-loaded liposomes. (**C**) Stability of blank and si-ITGA6-loaded liposomes in PBS for 24 h. (**D**) PDI of blank and si-ITGA6-loaded liposomes. (**E**) Zeta potential of blank and si-ITGA6-loaded liposomes. (**F**) CCK-8 assay results showed the toxicity of si-ITGA6-loaded liposomes in NIH3T3s. *p < 0.05, **p < 0.01, ****p < 0.0001.

of ITGA6 on fibroblasts and the anti-fibrotic effects of si-ITGA6. Further investigation demonstrated that ITGA6 regulated fibroblasts activity via FAK/PI3K/Akt signaling. Finally, the construction of si-ITGA6-loaded liposomes and in vivo experiments confirmed the potential application value of ITGA6-targeted therapy.

ACS is a common shoulder disorder with pain and stiffness.[4] Triggered by inflammation, this condition typically starts with pain and progresses to restricted active/passive ROM.[38] Pathologically, a substantial amount of fibroblasts migrate to the capsule in the inflammatory environment, and then secret a large amount of ECM, leading to capsule contracture, fibrosis, and stiffness.[26] The challenge in treating ACS stems from its unclear pathogenesis and the absence of effective therapeutic targets. The long-term efficacy of current treatments, such as physiotherapy and corticosteroid injections, remains to be explored.[39–41] In an effort to identify the potential therapeutic target for ACS, we collected capsule samples from patients with ACS, performing proteomic analysis on these samples, and ultimately selecting ITGA6 as a focal point for our research.

Integrins, as receptors on the cell surface, are crucial for biological processes such as cell adhesion, proliferation, and migration, which are related to pathological conditions including inflammation, fibrosis, healing, and metastasis.[42–44] Consequently, integrins and their signaling pathways are considered potential therapeutic targets for diseases such as cancer, inflammation, and fibrotic disorders.[45,46] It is already established that ITGA6 have a role in regulating disease progression by mediating cell adhesion, invasion, and migration.[47,48] Yuan et al reported that ITGA6 promoted fibroblast activation in pulmonary fibrosis.[35] Chen et al showed that ITGA6 mediated the invasion capability of matrix stiffness-regulated myofibroblast and led to lung fibrosis.[49] ITGB6 (integrin β6) was identified not only to be engaged in organ fibrosis but also be associated with cancer, periodontitis, and various potential genetic diseases.[50,51] Additionally, studies have shown that inhibition of integrins could significantly ameliorates fibrosis. Weinreb et al demonstrated that deletion or blockade of integrin αvβ6 had the potential to halt fibrosis progression or reverse established fibrosis in the mouse lung fibrosis model induced by bleomycin.[52] Ulmasov et al reported that blockade of integrin αv attenuated fibrosis in a mouse model of nonalcoholic steatohepatitis.[53] These findings suggest that integrins may serve as potential therapeutic targets for various fibrotic diseases. However, there is currently a lack of investigation on the regulatory role of integrins in the

https://doi.org/10.2147/IJN.S501561

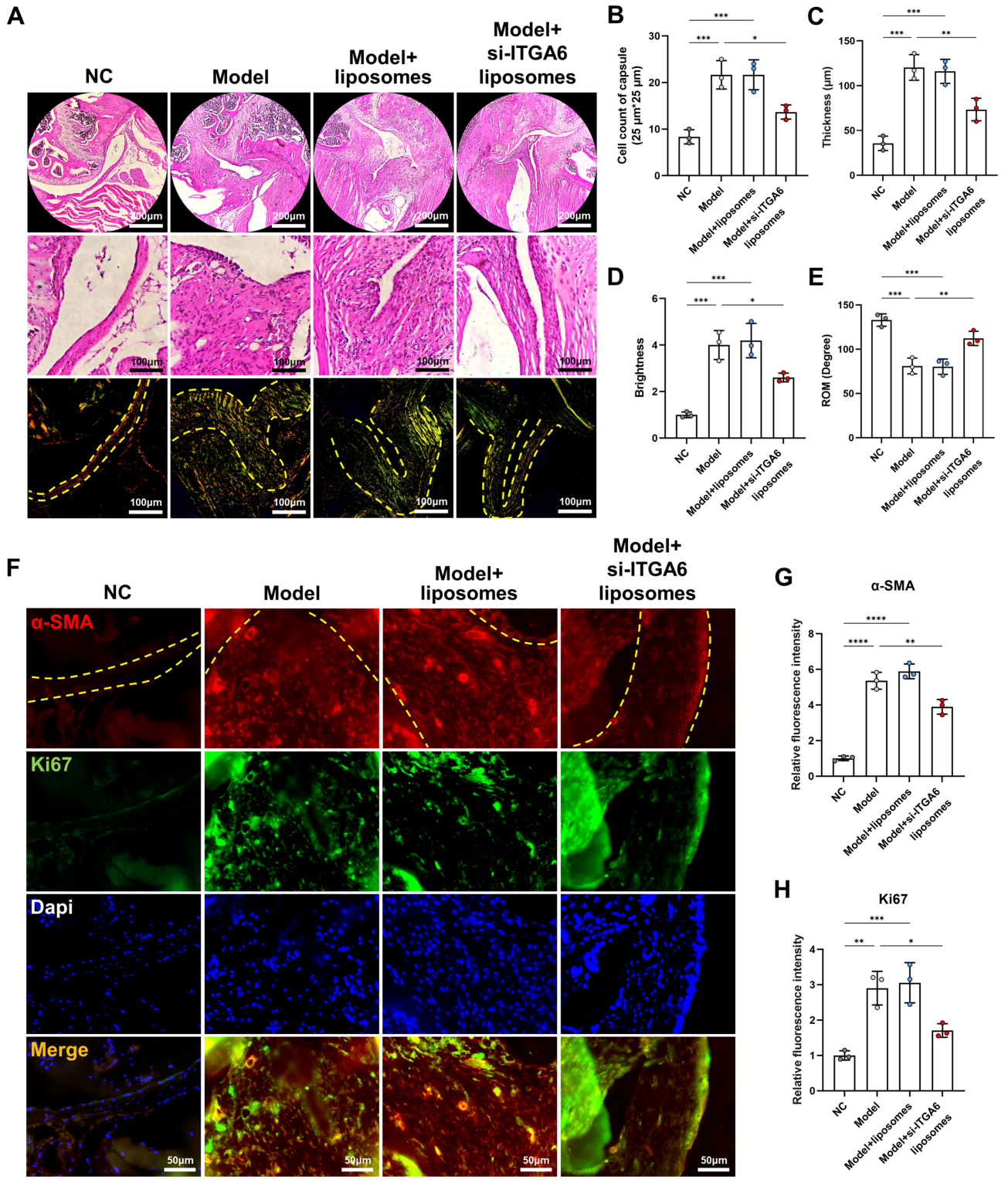

Figure 8 Si-ITGA6-loaded liposomes inhibited capsule fibrosis in vivo. (**A**) The representative HE and Sirius red staining images of the shoulder capsules in different group. The outline of the capsules was marked with yellow dashed lines. (**B**) Cell number in shoulder capsules. (**C**) Average capsule thickness. (**D**) Relative collagen deposition. (**E**) Passive range of motion of mice shoulder in different groups. (**F**–**H**) Immunofluorescence analysis of α-SMA and Ki67 in shoulder capsules. *p < 0.05, **p < 0.01, ***p<0.001, ****p < 0.0001.

pathogenesis and progression of ACS. In this study, we found that ITGA6 elevated significantly in the capsules of ACS patients and TGF-β induced CDFs/NIH3T3s. The inhibition of ITGA6 attenuated the viability, proliferation, and migration ability of fibroblasts, as well as fibrotic markers expression including Col 1, VIM, and α-SMA, indicating the regulatory role of ITGA6 on fibroblast activity.

FAK, a tyrosine kinase in the cytoplasm, is pivotal in the signal transduction processes mediated by integrins and activates multiple downstream signaling pathways.[54] The role of integrin signaling via FAK in regulating cell migration is well documented across various cell types, playing a significant part in the development of cancer and other diseases.[55,56] Additionally, the FAK/PI3K/Akt signaling pathway was reported to demonstrate a crucial regulatory role in fibrotic diseases,[36,57] which was consistent with our results. In this study, the overexpression of ITGA6 significantly enhanced the phosphorylation level of Akt, as well as the proliferation ability and fibrotic marker expression of CDFs. However, these results were reversed by the PI3K-Akt signaling inhibitor LY294002, indicating that ITGA6 regulated the activity and fibrotic phenotypes of CDFs through FAK/PI3K/Akt pathway.

In the in vivo experiments, the mouse ACS model was establishment through shoulder immobilization to simulated the conditions of ACS patients, including inflammatory cell infiltration, joint capsule thickening, and limited ROM, as described in previous studies.[10,30] Given the role of ITGA6 knockdown in inhibiting fibroblasts activity and fibrotic proteins expression, we opted for siRNA to specifically inhibit ITGA6. However, the in vivo application of siRNA-based therapy faces several challenges. One major obstacle is the delivery efficiency of siRNA to target cells, as siRNA can be rapidly degraded and has limited cellular uptake due to its negative charge and size,[58,59] and the activation of immune system caused by siRNA can result in inflammatory response.[60] Overcoming these obstacles requires the development of more efficient and safer delivery systems to enhance the therapeutic potential of siRNA.[61] In this study, we employed liposomes as carriers for si-ITGA6 considering the straightforward preparation, high translational potential, excellent biocompatibility, and superior encapsulation efficiency.[62] Liposome-based siRNA has emerged as a promising therapeutic strategy due to its enhanced stability, protection from degradation, and high efficiency of siRNA delivery. The liposomal membrane closely resembles cell membrane, facilitating the fusion with target cells via endocytosis, thereby enhancing intracellular uptake of siRNA.[22,63] Our results showed that the si-ITGA6-loaded liposomes significantly inhibited the expression of ITGA6 in the capsules of model mice and notably improved cell infiltration, capsule thickening, ROM, and capsule fibrosis. Furthermore, to determine the safe concentration of liposomes administered in mice, we assessed the impact of different concentration of si-ITGA6-loaded liposomes on cellular activity in murine fibroblasts NIH3T3s. These findings might provide the potential therapeutic application value of targeted therapy in ACS.

Still, there are several limitations. First, the limited number of clinical samples used for proteomic analysis might lead to biased results due to individual differences among patients. Second, the ACS model was conducted solely on young and healthy mice, while the onset of ACS can be triggered by various factors, such as rheumatoid arthritis, trauma, and diabetes.[3,64] Besides, mice, as quadrupedal animals, exhibit different shoulder joint movement patterns compared to those of humans. Therefore, additional animal models should be combined to validate our findings. Third, future studies should enhance the targeting specificity of liposomes towards fibroblasts through modifications to the liposomal membrane, thereby further improving the therapeutic efficacy.

Conclusions

In summary, our research revealed that ITGA6 was upregulated in capsules of ACS patients and was capable of enhancing fibroblast proliferation and migration abilities as well as promoting the expression of pro-fibrotic proteins via FAK/PI3K/Akt signaling pathway. By targeting ITGA6, si-ITGA6-loaded liposomes demonstrated the anti-fibrotic effect in capsule fibrosis. Integrin-targeted therapy demonstrated significant efficacy in various fibrotic diseases, exhibiting its value for broader clinical application. The limitations in current study include small sample size of proteomics and the use of single mouse model. Future researches should include more clinical samples and animal models as well as improve liposome targeting specificity. This study provides novel insights into the anti-fibrotic potential of ITGA6 targeted therapy, which may benefit patients with ACS in the future.

Data Sharing Statement

The datasets used and/or analysed during the current study are available from the corresponding author on reasonable request.

Ethics Approval and Informed Consent

The institutional ethical committee of Shanghai Pudong Hospital approved the current study (2022-RS-MS-06). All participants signed informed consent for shoulder capsule sample collection. This study was organized following the Declaration of Helsinki. All animal procedures were approved by the Institutional Animal Care and Use Committee of Shanghai Pudong Hospital, Fudan University (20231011-01).

Consent for Publication

Written informed consent was obtained from the patient for publication of this research.

Author Contributions

B.Q., Q.W., S.S. and Q.W. contributed equally to this work. All authors made a significant contribution to the work reported, whether that is in the conception, study design, execution, acquisition of data, analysis and interpretation, or in all these areas; took part in drafting, revising or critically reviewing the article; gave final approval of the version to be published; have agreed on the journal to which the article has been submitted; and agree to be accountable for all aspects of the work.

Funding

The study was supported by the Natural Science Foundation of Shanghai (Grant No. 22ZR1455800), Outstanding Leaders Training Program of Pudong Health Committee of Shanghai (Grant No. PWRI2021-01), Joint Research Project of Pudong Health Committee of Shanghai (Grant No. PW2021D-08), Program for the Outstanding Clinical Discipline Project of Shanghai Pudong (Grant No. PWYgy2021-04), the Leading Talent Project of Shanghai Pudong Hospital (Grant No. LJ202102, YJYJRC202102, KP9202101), the Project of Key Medical Specialty and Treatment Center of Pudong Hospital of Fudan University (Grant No. Zdzk2020-02, Zdzk2021-01), the National Natural Science Foundation of China (Grant No. 82102634), and the Science and Technology Development Foundation of Shanghai Pudong (Grant No. PKJ2022-Y48).

Disclosure

The authors declare that they have no competing interests.

References

1. Grey RG. The natural history of "idiopathic" frozen shoulder. *J Bone Joint Surg Am*. 1978;60(4):564.
2. Manske RC, Prohaska D. Diagnosis and management of adhesive capsulitis. *Curr Rev Musculoskelet Med*. 2008;1(3–4):180–189. doi:10.1007/s12178-008-9031-6
3. Koorevaar RCT, Van't Riet E, Ipskamp M, et al. Incidence and prognostic factors for postoperative frozen shoulder after shoulder surgery: a prospective cohort study. *Arch Orthop Trauma Surg*. 2017;137(3):293–301. doi:10.1007/s00402-016-2589-3
4. Zuckerman JD, Rokito A. Frozen shoulder: a consensus definition. *J Shoulder Elbow Surg*. 2011;20(2):322–325. doi:10.1016/j.jse.2010.07.008
5. Harris G, Bou-Haidar P, Harris C. Adhesive capsulitis: review of imaging and treatment. *J Med Imaging Radiat Oncol*. 2013;57(6):633–643. doi:10.1111/1754-9485.12111
6. Zhang L, Lou Q, Zhang W, et al. CircCAMTA1 facilitates atrial fibrosis by regulating the miR-214-3p/TGFBR1 axis in atrial fibrillation. *J Mol Histol*. 2023;54(1):55–65. doi:10.1007/s10735-022-10110-9
7. Rockey DC, Bell PD, Hill JA. Fibrosis–A Common Pathway to Organ Injury and Failure. *N Engl J Med*. 2015;373(1):96.
8. Henderson NC, Rieder F, Wynn TA. Fibrosis: from mechanisms to medicines. *Nature*. 2020;587(7835):555–566. doi:10.1038/s41586-020-2938-9
9. Hettrich CM, DiCarlo EF, Faryniarz D, et al. The effect of myofibroblasts and corticosteroid injections in adhesive capsulitis. *J Shoulder Elbow Surg*. 2016;25(8):1274–1279. doi:10.1016/j.jse.2016.01.012
10. Akbar M, McLean M, Garcia-Melchor E, et al. Fibroblast activation and inflammation in frozen shoulder. *PLoS One*. 2019;14(4):e0215301. doi:10.1371/journal.pone.0215301
11. Takase K. Oral steroid therapy for frozen shoulder. *West Indian Med J*. 2010;59(6):674–679.
12. D'Orsi GM, Via AG, Frizziero A, et al. Treatment of adhesive capsulitis: a review. *Muscles Ligaments Tendons J*. 2012;2(2):70–78.

13. Mertens MG, Meert L, Struyf F, et al. Exercise therapy is effective for improvement in range of motion, function, and pain in patients with frozen shoulder: a systematic review and meta-analysis. *Arch Phys Med Rehabil*. 2022;103(5):998–1012e14. doi:10.1016/j.apmr.2021.07.806
14. Wilkins MR, Sanchez JC, Gooley AA, et al. Progress with proteome projects: why all proteins expressed by a genome should be identified and how to do it. *Biotechnol Genet Eng Rev*. 1996;13:19–50. doi:10.1080/02648725.1996.10647923
15. Aebersold R, Mann M. Mass spectrometry-based proteomics. *Nature*. 2003;422(6928):198–207. doi:10.1038/nature01511
16. Goncalves E, Poulos RC, Cai Z, et al. Pan-cancer proteomic map of 949 human cell lines. *Cancer Cell*. 2022;40(8):835–849e8. doi:10.1016/j.ccell.2022.06.010
17. Elmas A, Lujambio A, Huang KL. Proteomic analyses identify therapeutic targets in hepatocellular carcinoma. *Front Oncol*. 2022;12:814120. doi:10.3389/fonc.2022.814120
18. Zhang T, Shi Y, Li J, et al. Utilize proteomic analysis to identify potential therapeutic targets for combating sepsis and sepsis-related death. *Front Endocrinol*. 2024;15:1448314. doi:10.3389/fendo.2024.1448314
19. Kohon MY, Zaaroor Levy M, Hornik-Lurie T, et al. alphavbeta3 integrin as a link between the development of fibrosis and thyroid hormones in systemic sclerosis. *Int J Mol Sci*. 2023;24(10):8927.
20. Zhang J, Wang T, Saigal A, et al. Discovery of a new class of integrin antibodies for fibrosis. *Sci Rep*. 2021;11(1):2118. doi:10.1038/s41598-021-81253-0
21. Ozpolat B, Sood AK, Lopez-Berestein G. Liposomal siRNA nanocarriers for cancer therapy. *Adv Drug Deliv Rev*. 2014;66:110–116. doi:10.1016/j.addr.2013.12.008
22. Zhang C, Tang N, Liu X, et al. siRNA-containing liposomes modified with polyarginine effectively silence the targeted gene. *J Control Release*. 2006;112(2):229–239. doi:10.1016/j.jconrel.2006.01.022
23. Hu B, Zhong L, Weng Y, et al. Therapeutic siRNA: state of the art. *Signal Transduct Target Ther*. 2020;5(1):101. doi:10.1038/s41392-020-0207-x
24. Chen J, Chen S, Li Y, et al. Is the extended release of the inferior glenohumeral ligament necessary for frozen shoulder? *Arthroscopy*. 2010;26(4):529–535. doi:10.1016/j.arthro.2010.02.020
25. Oh JH, Kim SH, Lee HK, et al. Moderate preoperative shoulder stiffness does not alter the clinical outcome of rotator cuff repair with arthroscopic release and manipulation. *Arthroscopy*. 2008;24(9):983–991. doi:10.1016/j.arthro.2008.06.007
26. Sun Y, Liu S, Chen S, et al. The effect of corticosteroid injection into rotator interval for early frozen shoulder: a randomized controlled trial. *Am J Sports Med*. 2018;46(3):663–670. doi:10.1177/0363546517744171
27. Yang R, Deng H, Hou J, et al. Investigation of salmon calcitonin in regulating fibrosis-related molecule production and cell-substrate adhesion in frozen shoulder synovial/capsular fibroblasts. *J Orthop Res*. 2020;38(6):1375–1385. doi:10.1002/jor.24571
28. Qi B, Li Y, Peng Z, et al. Macrophage-myofibroblast transition as a potential origin for skeletal muscle fibrosis after injury via complement system activation. *J Inflamm Res*. 2024;17:1083–1094. doi:10.2147/JIR.S450599
29. Sun Y, Luo Z, Chen Y, et al. si-Tgfbr1-loading liposomes inhibit shoulder capsule fibrosis via mimicking the protective function of exosomes from patients with adhesive capsulitis. *Biomater Res*. 2022;26(1):39. doi:10.1186/s40824-022-00286-2
30. Kanno A, Sano H, Itoi E. Development of a shoulder contracture model in rats. *J Shoulder Elbow Surg*. 2010;19(5):700–708. doi:10.1016/j.jse.2010.02.004
31. Villa-Camacho JC, Okajima S, Perez-Viloria ME, et al. In vivo kinetic evaluation of an adhesive capsulitis model in rats. *J Shoulder Elbow Surg*. 2015;24(11):1809–1816. doi:10.1016/j.jse.2015.06.015
32. Oki S, Shirasawa H, Yoda M, et al. Generation and characterization of a novel shoulder contracture mouse model. *J Orthop Res*. 2015;33(11):1732–1738. doi:10.1002/jor.22943
33. Munger JS, Huang X, Kawakatsu H, et al. The integrin alpha v beta 6 binds and activates latent TGF beta 1: a mechanism for regulating pulmonary inflammation and fibrosis. *Cell*. 1999;96(3):319–328. doi:10.1016/S0092-8674(00)80545-0
34. Margadant C, Sonnenberg A. Integrin-TGF-beta crosstalk in fibrosis, cancer and wound healing. *EMBO Rep*. 2010;11(2):97–105. doi:10.1038/embor.2009.276
35. Yuan J, Li P, Pan H, et al. miR-542-5p attenuates fibroblast activation by targeting integrin alpha6 in silica-induced pulmonary fibrosis. *Int J Mol Sci*. 2018;19(12):3717. doi:10.3390/ijms19123717
36. Huang Y, Zhao H, Zhang Y, et al. Enhancement of zyxin promotes skin fibrosis by regulating FAK/PI3K/AKT and TGF-beta signaling pathways via integrins. *Int J Biol Sci*. 2023;19(8):2394–2408. doi:10.7150/ijbs.77649
37. Liu P, Chen G, Zhang J. A review of liposomes as a drug delivery system: current status of approved products, regulatory environments, and future perspectives. *Molecules*. 2022;27(4).
38. Chen J, Zhu J, Zhu T, et al. Pathological changes of frozen shoulder in rat model and the therapeutic effect of PPAR-gamma agonist. *J Orthop Res*. 2021;39(4):891–901. doi:10.1002/jor.24920
39. Rhind V, Downie WW, Bird HA, et al. Naproxen and indomethacin in periarthritis of the shoulder. *Rheumatol Rehabil*. 1982;21(1):51–53. doi:10.1093/rheumatology/21.1.51
40. Zhang J, Zhong S, Tan T, et al. Comparative efficacy and patient-specific moderating factors of nonsurgical treatment strategies for frozen shoulder: an updated systematic review and network meta-analysis. *Am J Sports Med*. 2021;49(6):1669–1679. doi:10.1177/0363546520956293
41. Mertens MG, Meeus M, Verborgt O, et al. An overview of effective and potential new conservative interventions in patients with frozen shoulder. *Rheumatol Int*. 2022;42(6):925–936. doi:10.1007/s00296-021-04979-0
42. Hynes RO. Integrins: a family of cell surface receptors. *Cell*. 1987;48(4):549–554. doi:10.1016/0092-8674(87)90233-9
43. Hynes RO, Yamada KM. Fibronectins: multifunctional modular glycoproteins. *J Cell Biol*. 1982;95(2 Pt 1):369–377. doi:10.1083/jcb.95.2.369
44. Kechagia JZ, Ivaska J, Roca-Cusachs P. Integrins as biomechanical sensors of the microenvironment. *Nat Rev Mol Cell Biol*. 2019;20(8):457–473. doi:10.1038/s41580-019-0134-2
45. Slack RJ, Macdonald SJF, Roper JA, et al. Emerging therapeutic opportunities for integrin inhibitors. *Nat Rev Drug Discov*. 2022;21(1):60–78. doi:10.1038/s41573-021-00284-4
46. Pang X, He X, Qiu Z, et al. Targeting integrin pathways: mechanisms and advances in therapy. *Signal Transduct Target Ther*. 2023;8(1):1. doi:10.1038/s41392-022-01259-6
47. Jandova J, MASON CJ, PAWAR SC, et al. Fn14 receptor promotes invasive potential and metastatic capacity of non-small lung adenocarcinoma cells through the up-regulation of integrin alpha6. *Neoplasma*. 2015;62(1):41–52. doi:10.4149/neo_2015_006

48. Ramovs V, Te Molder L, Sonnenberg A. The opposing roles of laminin-binding integrins in cancer. *Matrix Biol*. 2017;57-58:213–243. doi:10.1016/j.matbio.2016.08.007
49. Chen H, Qu J, Huang X, et al. Mechanosensing by the alpha6-integrin confers an invasive fibroblast phenotype and mediates lung fibrosis. *Nat Commun*. 2016;7:12564. doi:10.1038/ncomms12564
50. Zhang Z, Wang Z, Liu T, et al. Exploring the role of ITGB6: fibrosis, cancer, and other diseases. *Apoptosis*. 2024;29(5–6):570–585. doi:10.1007/s10495-023-01921-6
51. Koivisto L, Bi J, Häkkinen L, et al. Integrin alphavbeta6: structure, function and role in health and disease. *Int J Biochem Cell Biol*. 2018;99:186–196. doi:10.1016/j.biocel.2018.04.013
52. Weinreb PH, Simon KJ, Rayhorn P, et al. Function-blocking integrin alphavbeta6 monoclonal antibodies: distinct ligand-mimetic and nonligand-mimetic classes. *J Biol Chem*. 2004;279(17):17875–17887. doi:10.1074/jbc.M312103200
53. Ulmasov B, Noritake H, Carmichael P, et al. An inhibitor of arginine-glycine-aspartate-binding integrins reverses fibrosis in a mouse model of nonalcoholic steatohepatitis. *Hepatol Commun*. 2019;3(2):246–261. doi:10.1002/hep4.1298
54. Zhao X, Guan JL. Focal adhesion kinase and its signaling pathways in cell migration and angiogenesis. *Adv Drug Deliv Rev*. 2011;63(8):610–615. doi:10.1016/j.addr.2010.11.001
55. McLean GW, Carragher NO, Avizienyte E, et al. The role of focal-adhesion kinase in cancer - a new therapeutic opportunity. *Nat Rev Cancer*. 2005;5(7):505–515. doi:10.1038/nrc1647
56. Golubovskaya VM, Cance WG. Focal adhesion kinase and p53 signaling in cancer cells. *Int Rev Cytol*. 2007;263:103–153. doi:10.1016/S0074-7696(07)63003-4
57. Qi X, Chen Y, Liu S, et al. Sanguinarine inhibits melanoma invasion and migration by targeting the FAK/PI3K/AKT/mTOR signalling pathway. *Pharm Biol*. 2023;61(1):696–709. doi:10.1080/13880209.2023.2200787
58. Whitehead KA, Langer R, Anderson DG. Knocking down barriers: advances in siRNA delivery. *Nat Rev Drug Discov*. 2009;8(2):129–138. doi:10.1038/nrd2742
59. Tezgel O, Szarpak-Jankowska A, Arnould A, et al. Chitosan-lipid nanoparticles (CS-LNPs): application to siRNA delivery. *J Colloid Interface Sci*. 2018;510:45–56. doi:10.1016/j.jcis.2017.09.045
60. Sajid MI, Moazzam M, Kato S, et al. Overcoming barriers for siRNA therapeutics: from bench to bedside. *Pharmaceuticals*. 2020;13(10).
61. Xue HY, Liu S, Wong HL. Nanotoxicity: a key obstacle to clinical translation of siRNA-based nanomedicine. *Nanomedicine*. 2014;9(2):295–312. doi:10.2217/nnm.13.204
62. Pan T, Zhou Q, Miao K, et al. Suppressing Sart1 to modulate macrophage polarization by siRNA-loaded liposomes: a promising therapeutic strategy for pulmonary fibrosis. *Theranostics*. 2021;11(3):1192–1206. doi:10.7150/thno.48152
63. Huang Y, Zheng S, Guo Z, et al. Ionizable liposomal siRNA therapeutics enables potent and persistent treatment of Hepatitis B. *Signal Transduct Target Ther*. 2022;7(1):38. doi:10.1038/s41392-021-00859-y
64. Konarski W, Poboży T, Hordowicz M, et al. Current concepts of natural course and in management of frozen shoulder: a clinical overview. *Orthop Rev*. 2020;12(4):8832.